CrossMark

ORIGINAL PAPER

Oxidovanadium(IV) complexes with chrysin and silibinin: anticancer activity and mechanisms of action in a human colon adenocarcinoma model

I. E. León[1,2] · J. F. Cadavid-Vargas[1,2] · I. Tiscornia[3] · V. Porro[3] · S. Castelli[4] ·
P. Katkar[4] · A. Desideri[4] · M. Bollati-Fogolin[3] · S. B. Etcheverry[1,2]

Abstract Vanadium compounds were studied during recent years to be considered as a representative of a new class of nonplatinum metal antitumor agents in combination to its low toxicity. On the other hand, flavonoids are a wide family of polyphenolic compounds synthesized by plants that display many interesting biological effects. Since coordination of ligands to metals can improve the pharmacological properties, we report herein, for the first time, a exhaustive study of the mechanisms of action of two oxidovanadium(IV) complexes with the flavonoids: silibinin $Na_2[VO(silibinin)_2]\cdot6H_2O$ (VOsil) and chrysin $[VO(chrysin)_2EtOH]_2$ (VOchrys) on human colon adenocarcinoma derived cell line HT-29. The complexes inhibited the cell viability of colon adenocarcinoma cells in a dose dependent manner with a greater potency than that the free ligands and free metal, demonstrating the benefit of complexation. The decrease of the ratio of the amount of reduced glutathione to the amount of oxidized glutathione were involved in the deleterious effects of both complexes. Besides, VOchrys caused cell cycle arrest in G2/M phase while VOsil activated caspase 3 and triggering the cells directly to apoptosis. Moreover, VOsil diminished the NF-kB activation via increasing the sensitivity of cells to apoptosis. On the other hand, VOsil inhibited the topoisomerase IB activity concluding that this is important target involved in the anticancer vanadium effects. As a whole, the results presented herein demonstrate that VOsil has a stronger deleterious action than VOchrys on HT-29 cells, whereby suggesting that Vosil is the potentially best candidate for future use in alternative anti-tumor treatments.

Graphical Abstract
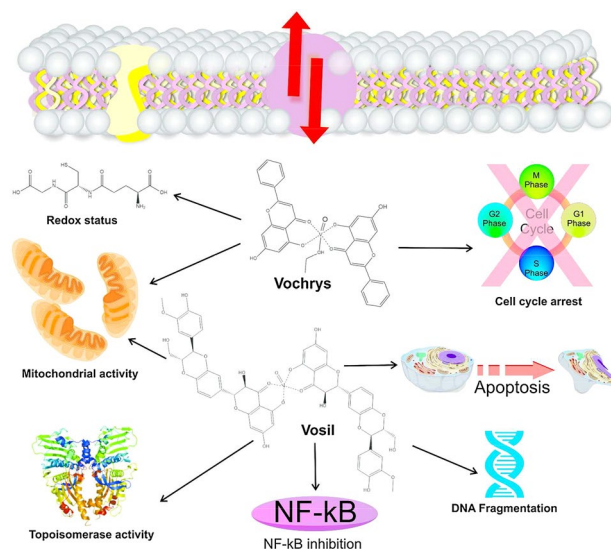
✉ S. B. Etcheverry
etcheverry@biol.unlp.edu.ar

1 Cátedra de Bioquímica Patológica, Facultad Ciencias Exactas, Universidad Nacional de La Plata, 47 y 115, 1900 La Plata, Argentina

2 Centro de Química Inorgánica (CEQUINOR-CONICET), Facultad de Ciencias Exactas, Universidad Nacional de La Plata, 47 y 115, 1900 La Plata, Argentina

3 Unidad de Biología Celular, Institut Pasteur de Montevideo, Mataojo 2020, 11400 Montevideo, Uruguay

4 Department of Biology, University of Rome "Tor Vergata", Rome, Italy

Springer

Introduction

Colon cancer is one of the main causes of cancer-associated deaths worldwide [1]. The incidence of colon cancer is strongly related to lifestyle, particularly dietary habits [2]. Several drugs can be used to treat colorectal cancer such as irinotecan, 5-fluorouracil (5-FU) and oxaliplatin. The principal problems of this type of drugs are the side effects such as nausea, vomiting, loss of appetite, adverse effects on blood-forming cells and resistance. Therefore, in the last decade, different scientific groups have made many efforts to obtain new metallo-compounds that improve the antitumor properties and diminish the side effects against colon cancer.

Vanadium is an ultratrace element with interesting pharmacological properties present in animals and higher plants [3]. The pharmacological actions of vanadium convert its compounds into potential therapeutic agents to be used in the treatment of a number of diseases. In particular, vanadate(V) and vanadyl(IV) derivatives show insulin-mimetic/antidiabetic activity [4, 5], neurologic [6] and anticancer effects [7]. In this sense, the anticancer effects of vanadium complexes have been widely investigated on various types of tumor cell lines. Several vanadium compounds inhibit the cell cycle and can also inhibit cell proliferation even at low doses [8, 9]. Recently, vanadium compounds have been considered as a new class of non-platinum metal-based antitumor agents [8, 10]. Several mechanisms have been described to explain the cell cycle arrest and the induction of tumor cell death by vanadium derivatives. In particular, the generation of ROS may cause a series of effects such as protein tyrosine phosphatase inhibition, DNA cleavage, oxidative damage of cellular components and finally trigger apoptosis [7].

Nevertheless, since inorganic vanadium compounds are poorly absorbed and cause gastrointestinal problems,

several research groups have synthesized complexes of vanadium with organic ligands, such as flavonoids but their biological properties were have not been completely examined [11, 12]. Flavonoids are a large family of compounds synthesized by plants that have a common chemical structure [13]. Last few decades, there has been an increased interest in the utility of flavonoids based upon their broad spectrum of biological properties, including cardioprotective, antioxidative and anticarcinogenic activities [14].

Within the members of flavonoid family are silibinin and chrysin. Silibinin (3,5,7-trihydroxy-2-[3-(S)-(4-hydroxy-3-methoxyphenyl)-2-(S)-(hydroxymethyl)-2,3-dihydro-1,4-benzodioxin-6-yl]chroman-4-one) (Fig. 1a), a flavonol-ignan isolated from milk thistle seeds, is the major active constituent of silymarin and one of the popular dietary supplements that has been extensively studied for its hepatoprotective, antioxidant and antitumor properties [12]. Silibinin has also demonstrated potent anticancer effects against various tumor types such as breast and pancreas. [15–17].

On the other hand, chrysin, 5,7-dihydroxy-2-phenyl-4H-chromen-4-one (Fig. 1b), is a naturally occurring flavone extracted from the honeycomb and blue passion flower [18]. The antitumor effects of chrysin have been previously reported in several tumor cell lines [19–21]. Coordination of the inorganic vanadium species with organic molecules may improve their solubility, stability, transport and absorption [22–24]. These aspects are very important when considering treatments with high doses of the compounds or when long time exposures are needed [25, 26]. Besides, the biological effects of vanadium complexes are more effective than those of free flavonoids, meaning that the physiological and anticancer properties of flavonoids are enhanced on complexation [27, 28].

As part of a project related to vanadium compounds with potential pharmacological applications in cancer, the present study deals with the effects of an oxovanadium(IV) complexes with the flavonoids silibinin $Na_2[VO(silibinin)_2]\cdot 6H_2O$ (VOsil) and chrysin $[VO(chrysin)_2EtOH]_2$ (VOchrys) on a human colorectal adenocarcinoma cell line (HT-29). We have investigated
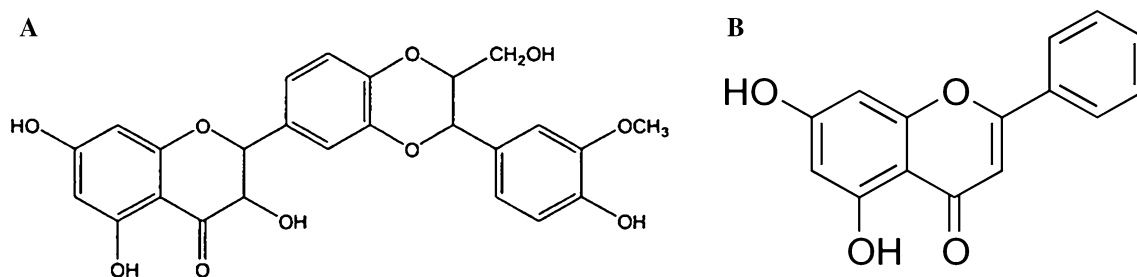
Fig. 1 Chemical structure of silibinin, 3,5,7-trihydroxy-2-[3-(S)-(4-hydroxy-3-methoxyphenyl)-2-(S)-(hydroxymethyl)-2,3-dihydro-1,4-benzo-dioxin-6-yl]chroman-4-one and chrysin, 5,7-dihydroxy-2-phenyl-4H-chromen-4-one

and reported herein, the effects of the complexes on cell viability of this tumor cell line and the putative mechanisms involved in their anticancer effects. In particular, we focus our investigation on the cellular redox status, its effects on cytotoxicity and mitochondria metabolism, as well as on the cell cycle arrest, apoptosis and NF-kB via inhibition. Finally, we have investigated the effect of these compounds on the human topoisomerase activity.

Experimental

Materials

Tissue culture materials were purchased from Corning (Princeton, NJ, USA), Dulbecco's Modified Eagles Medium (DMEM), TrypLE™ from Gibco (Gaithersburg, MD, USA), and fetal bovine serum (FBS) from Internegocios SA (Argentina). Annexin V, Fluorescein isothiocyanate (FITC)/PI, tetrazolium salt MTT (3-(4, 5-dimethylthiazol-2-yl)-2,5-diphenyl-tetrazolium-bromide) from Invitrogen Corporation (Buenos Aires, Argentina). The caspase-3 assay was achieved by commercial kit (Caspase 3 Assay Kit Pharmingen™ BD).

All other chemical were from Sigma Chemical Co. (ST. Louis, MO, USA).

Methods

Synthesis and identification of VOsil and VOchrys

VOsil and VOchrys were synthesized according to previously reported results [11, 12].

The identification of the complexes was done using FTIR.

Preparation of VOsil and VOchrys solutions

Fresh stock solutions of the complexes and the free ligands were prepared in DMSO at 20 mM and diluted according to the concentrations indicated in the legends of the figures. Precautions should be taken with the maximum concentration of DMSO in the well plate. We used 0.5 % as the maximum DMSO concentration to avoid toxic effects of this solvent for the cells.

Cell culture and incubations

HT-29 cell line was purchased from *ATCC* (HTB-38™).

HT-29 and HT-29 NFκB-hrGFP cells were grown in DMEM and RPMI 1640 containing 10 % FBS, 100 U/mL penicillin and 100 μg/mL streptomycin at 37 °C in 5 % CO_2 atmosphere. Cells were seeded in a 25-cm^2 flask and when 70–80 % of confluence was reached, cells were subcultured using 1 mL of TrypLE™ per 25 cm^2 flask. For

experiments, cells were grown in multi-well plates. When cells reached the desired confluence, the monolayers were washed with DMEM and were incubated under different conditions according to the experiments.

Cell viability: crystal violet assay

A mitogenic bioassay was carried out as described by Okajima et al. [29] with some modifications. In brief, cells were grown in 48-well plates. For experiments, the cells (3×10^4 cells/mL) were grown for 24 h at 37 °C. Then, for the viability assay, the monolayer was incubated with different concentrations (2.5–100 μM) of the free ligand or the complex. After this treatment, the monolayers were washed with PBS and fixed with 5 % glutaraldehyde/PBS at room temperature for 10 min. After that, they were stained with 0.5 % crystal violet/25 % methanol for 10 min. Then, the dye solution was discarded and the plate was washed with water and dried. The dye taken up by the cells was extracted using 0.5 mL/well 0.1 M glycine/HCl buffer, pH 3.0/30 % methanol and transferred to test tubes. Absorbance was read at 540 nm after a convenient sample dilution. It was previously shown that under these conditions, the colorimetric bioassay strongly correlated with cell proliferation measured by cell counting in Neubauer chamber [30].

MTT assay

The MTT assay was based on a report previously described by Mosmann [31]. In brief, cells were seeded in a 96-multiwell dish, allowed to attach for 24 h and treated with different concentrations of complexes at 37 °C for 24 h. After this treatment, the medium was changed and the cells were incubated with 0.5 mg/mL MTT under normal culture conditions for 3 h. Cell viability was marked by the conversion of the tetrazolium salt MTT (3-(4, 5-dimethylthiazol-2-yl)-2,5-diphenyl-tetrazolium-bromide) to a colored formazan by mitochondrial dehydrogenases. Color development was measured spectrophotometrically in a Microplate Reader (7530, Cambridge technology, Inc, USA) at 570 nm after cell lysis in DMSO (100 μL/well). Cell viability is shown graphically as the percentage of the control value.

Neutral red assay

The neutral red (NR) accumulation assay was performed according to Borenfreund and Puerner [32]. Cells were seeded in 96-well culture plates at a ratio of 2.5×10^4 cells per well. Cells were treated with different VOsil/VOchrys concentrations for 24 h at 37 °C in 5 %CO_2 in air.

After treatment, the medium was replaced by one containing 100 μg/mL NR dye, and the cells were incubated for 3 h. Then, the NR medium was discarded, the cells were rinsed twice with prewarmed (37 °C) PBS to remove the non incorporated dye, and 100 μL of 50 % ethanol/1 % acetic acid solution was added to each well to fix the cells, releasing the NR into solution. The plates were shaken for

10 min, and the absorbance of the solution was measured with a microplate reader (model 7530, Cambridge Technology, USA) at 540 nm. The optical density was plotted as the percentage of the optical density of the control.

Fluorometric determination of cellular GSH and GSSG levels GSH and GSSG levels were determined in cells in culture as follows. Confluent HT-29 monolayers from 24-well dishes were incubated with different concentrations of both complexes at 37 °C for 24 h. Then, the monolayers were washed with PBS and harvested by incubating them with 250 µL Triton 0.1 % for 30 min. For GSH determination, 100 µL aliquots were mixed with 1.8 mL of ice-cold phosphate buffer (Na_2HPO_4 0.1 M-EDTA 0.005 M pH 8) and 100 µL o-phthaldialdehyde (0.1 % in methanol) as it was described by Hissin and Hilf [33]. For the determination of GSSG, 100 µL aliquots were mixed with 1.8 mL NaOH 0.1 M and o-phthaldialdehyde as before. Previously, to avoid GSH oxidation, the cellular extracts for GSSG determination were incubated with 0.04 M of *N*-ethylmaleimide (NEM). Fluorescence at an emission wavelength of 420 nm was determined after excitation at 350 nm.

The ratio GSH/GSSG, which is a better marker for the cellular redox status, was calculated as percentage basal for all the experimental conditions.

On the other hand, the change in cellular redox potential were calculated using the Nernst´s equation for the reduction potential of the GSSG/2GSH half-cell

$$E_{hc} = -264 - (59.1/2)\log\left([GSH]^2/[GSSG]\right) \text{ mV at } 25°C, \text{ pH } 7.4.$$

The pH condition used to calculate the E_{hc} values is the same of pH of DMEM medium used for cell culture.

Measurement of the exposure of phosphatidyl serine (PS) by annexin V-FITC/PI staining Cells in early and late stages of apoptosis were detected with Annexin V-FITC and propidium iodide (PI) staining. Cells were treated with 100 µM VOsil and VOchrys incubated for 6 and 24 h prior to analysis. For the staining, cells were washed with PBS and adjusted to a concentration of 1×10^6 cell/mL in $1\times$ binding buffer. To 100 µL of cell suspension, 2.5 µL of Annexin V-FITC and 2 µL PI (250 µg/mL) were added and incubated for 15 min at room temperature prior to analysis. Cells were analyzed using flow cytometer CyAnTM ADP (Beckman Coulter, USA) and Summit v4.3 software. For each analysis, 10,000 counts, gated on a FSC vs SSC dot plot, were recorded. Four subpopulations were defined in the dot plot: the undamaged vital (Annexin V−/PI−), the vital mechanically damaged (Annexin V−/PI+), the apoptotic (Annexin V+/PI−), and the secondary necrotic (Annexin V+/PI+) subpopulations.

Caspase 3 assay The determination of caspase 3, one of the main effector caspases, was carried out with a commercial kit (Caspase 3 Assay Kit Pharmingen™, BD) following the recommendations of manufacturers.

In brief, cells were grown in 24-well plates for 24 h (3×10^5 cells/well). Then, the monolayer was incubated with 100 µM of the complexes for 6 h. After this treatment, the monolayers were washed with PBS and were harvested with TrypLE™ at 37 °C for 5 min.

After that, cytofix/cytoperm buffer $1\times$ was added and incubated in an ice-cold bath for 20 min. Then, the tubes were centrifuged at 1000 rpm for 5 min and the cells were collected. After that, anti caspase-3 FITC antibody was added and incubated for 30 min at room temperature. Then, the cells were analyzed using flow cytometer CyAnTM ADP (Beckman Coulter, USA) and Summit v4.3 software.

Measurement of cell cycle/DNA content DNA content in G_1/G_0, S, G_2/M phases was analyzed using flow cytometry [34]. Cells were seeded on 6-well plates, cultured during 24 h and then treated with 100 µM of complexes for 24 and 48 h. The harvested cells were washed with PBS, fixed and permeabilized with 70 % ice-cold ethanol for more than 2 h. Subsequently, cells were resuspended in freshly staining buffer (15 mg/mL of PI and 15 mg/mL DNase-free RNase prepared in PBS containing 2 mM EDTA) and incubated for 15 min at 37 °C. After gating out cellular aggregates, the cell cycle distribution analysis was performed on CyAnTM ADP flow cytometer using Summit v4.3 software for the acquisition. For each sample, at least 10,000 cells were counted and plotted on a single parameter histogram. The percentage of cells in the G_1/G_0, S, G_2/M phases and sub-G_1 peak was then calculated using FlowJo 7.6 software (Watson model).

NF-κB pathway inhibition assay HT-29-NF-κB-hrGFP reporter cells [35] were seeded in 96-well plates (5.0×10^4cells/well) in RPMI 1640 supplemented with 10 % (v/v) heat-inactivated fetal calf serum. After 24 h, the medium was renewed and 25 and 50 µM of both complexes were added 2 h before stimulation with 3 ng/mL of TNF-α. Three controls were included: (1) cells treated only with complete RPMI 1640 medium; (2) cells treated only with TNF-α; and (3) cells treated with DMSO 0.5 %. Cells were incubated for 18 h at 37 °C in a 5 % CO_2 humidified atmosphere and finally trypsinized for flow cytometry analysis. Cells were analyzed using a CyAn™ ADP (Beckman Coulter, USA) flow cytometer equipped with 488 nm and 635 nm lasers. Summit 4.3 software was used for data acquisition and analysis. Green fluorescence protein (GFP) and propidium iodide (PI) fluorescence emissions were detected by band-pass filter 530/40 and 613/20, respectively, employing a logarithmic scale. For each sample, 10,000 counts gated on a FSC vs SSC dot plot, excluding doublets were

recorded. Only single living cells (cells that excluded PI) were considered for results' comparison and the percentage of GFP positive cells were normalized against the percentage of GFP cells obtained with the TNF-α.

Purification of human topoisomerase IB Human topoisomerase IB was expressed under the galactose inducible promoter in a multi-copy plasmid, YEpGAL1-e-wild type and YEpGAL1-e-Y723F, used for transformation of EKY3 cells, as described previously by Chillemi and col [36]. The epitope-tagged constructs contain the N-terminal sequence FLAG: DYKDDDY (indicated with "e"), recognized by the M2 monoclonal antibody. The purification was carried out using the ANTI-FLAG M2 Affinity Gel column. FLAG-fusion topoisomerase IB was eluted by competition with five column volumes of a solution containing 100 μg/ml FLAG peptide in 50 mM Tris–HCl, 150 mM KCl pH 7.4. Glycerol was added into each collected fraction up to a final concentration of 33 %; all the fractions were stored at 20 °C. One aliquot from each single fraction was resolved by SDS–polyacrylamide gel electrophoresis; using the epitope-specific monoclonal antibody M2 protein, concentration and integrity were measured through immunoblot assay.

DNA relaxation assays The activity of topoisomerase IB was assayed in 20 μL of reaction volume containing 0.5 μg of negatively supercoiled pBlue-Script KSII(+) DNA and Reaction Buffer (20 mM Tris–HCl, 0.1 mM Na_2EDTA, 10 mM $MgCl_2$, 50 μg/ml acetylated BSA and 150 mM KCl, pH 7.5). The effect of the complexes on enzyme activity was measured by adding different concentrations of the compounds, at different times. Reactions were stopped with a final concentration of 0.5 % SDS after 30 min or after each time-course point at 37 °C. The samples were electrophoresed in a horizontal 1 % agarose gel in 50 mM Tris, 45 mM boric acid, 1 mM EDTA). The gel was stained with ethidium bromide (5 μg/mL), destained with water and photographed under UV illumination. Where indicated, enzyme and inhibitor were preincubated at 37 °C for 5 min, prior to the addition of the substrate. Assays were performed at least three times but only one representative gel is shown.

Cleavage kinetics The oligonucleotide substrate CL14 (50-GAAAAAAGACTTAG-30) radiolabelled with [g-32P] ATP at its 50 end and the CP25 complementary strand (50-TAAAAATTTTTCTAAGTCTTTTTTC-30), phosphorylated at its 50 end with unlabeled ATP, were annealed at a twofold molar excess of CP25 over CL14, creating the so-called "suicide substrate", which contains only a partial duplex. The suicide cleavage reactions were performed incubating 20 nM of this partial duplex substrate with an excess of enzyme in reaction buffer at 37 °C and in the presence of 150 μM of VOsil. DMSO was added to no-drug

control. When indicated, VOsil was pre-incubated with the enzyme for 5 min before the addition of a DNA substrate. Previous to the addition of the enzyme, a 5-ml sample of the reaction mixture was removed and used as the zero time point. At different time points, 5-ml aliquots were removed and the reaction stopped with 0.5 % SDS. After ethanol precipitation, the samples were re-suspended in 6 μL of 1 mg/mL trypsin and incubated at 37 °C for 1 h. Samples were analyzed using denaturing urea/polyacrylamide gel electrophoresis. Each experiment was replicated at least three times and a representative gel is shown.

Religation kinetics A suicide CL14/CP25 substrate (20 nM), prepared as above, was incubated with an excess of topoisomerase IB enzyme for 30 min at 37 °C in reaction Buffer. A 5-ml sample of the reaction mixture was removed and used as the zero time point. Religation reactions were initiated by adding a 200-fold molar excess of R11 oligonucleotide (50-AGAAAAATTTT-30) over the duplex CL14/CP25 in the presence or absence of 150 μM of VOsil. At different times, 5 mL aliquots were removed and the reaction stopped with 0.5 % SDS. After ethanol precipitation, the samples were re-suspended in 5 mL of 1 mg/mL trypsin and incubated at 37 °C for 30 min. Samples were analyzed by denaturing urea/polyacrylamide gel electrophoresis. Each experiment was replicated three times and a representative gel is shown.

Electrophoretic mobility-shift assay (EMSA) This assay was done using the same double-stranded 25 bp oligonucleotide CL25/CP25 prepared for the cleavage/equilibrium assay. The reactions were carried out using the catalytically inactive mutant Y723F. The mutant enzyme was incubated in standard reaction conditions [20 mM Tris–HCl, pH 7.5, 0.1 mM Na_2EDTA, 10 mM $MgCl_2$, 50 μg/mL acetylated BSA and 150 mM KCl] in the presence of 1 % (v/v) DMSO, 150 μM VOsil at 37 °C for 30 min in a final volume of 20 μL. In the case of pre-incubation, the enzyme was incubated with VOsil for 5 min before adding the DNA substrate and letting the binding reactions proceed for 30 min at 37 °C. Reactions were stopped by the addition of 5 μL of dye [0.125 % Bromophenol Blue and 40 % (v/v) glycerol]. Samples were loaded onto 6 % (v/v) native polyacrylamide gels and electrophoresed at 40 V in TBE3 (12 mM Tris, 11.4 mM boric acid and 0.2 mM EDTA) at 4 °C for 4 h. Products were visualized by PhosphorImager.

Statistical analysis

At least three independent experiments were performed for each experimental condition in all the biological assays. The results are expressed as the mean ± the standard error of the mean (SEM). Statistical differences were analyzed

using the analysis of variance method (ANOVA) followed by the test of least significant difference (Fisher).

Results and discussion

Results

Synthesis, identification and active species of VOchrys and VOsil

VOchrys and VOsil were synthesized according to Naso et al. [11, 12]. The method is briefly described in the Materials and Methods section. The obtained powder sample of each complex was identified by FTIR and the main vibrations of the organic moiety were compared. Besides, it was assumed that in the proposed complex structure for VOchrys, the axial positions were occupied by the oxygen atom of VO and the other axial position by a solvent molecule. The equatorial positions are occupied by two organic ligand molecules. Besides, for VOsil, it can be seen that the binding mode of this complex could be expected to involve an equatorial coordination sphere with two deprotonated ArO– (from the flavonoid moiety) and two oxygen atoms from C=O groups bound to the oxovanadium(IV) center [11, 12].

Effect of chemical complexation on cell viability

To test the effect of chemical complexation on cell viability, human HT-29 colorectal adenocarcinoma

cells were exposed to the flavonoids silibinin, chrysin, the oxidovanadium(IV) cation, and the complexes VOchrys and VOsil. As can be seen in Fig. 2, the oxidovanadium(IV) cation provoked an inhibitory effect only at 100 μM, whereas silibinin and chrysin did not show effects in this cell line. On the contrary, VOsil and VOchrys impaired cell viability from 75 μM ($p < 0.01$). Moreover, the antiproliferative action of the complexes are much stronger than the effects of the vanadyl(IV) cation and free flavonoids in the whole range of the studied concentrations ($p < 0.01$), demonstrating an improvement of the anticancer action through the complexation of chrysin and silibinin with vanadyl(IV).

To determine the antitumor effectiveness of both complexes, we compared their effects with those of the reference metal-based drug (cisplatin) in HT-29 cells. Figure 3 shows the effects of VOchrys, VOsil and cisplatin (CDDP) on the cell viability of HT-29 cells. As it can be seen, CDDP caused an inhibitory effect only at 100 μM, while VOchrys and VOsil provoked antitumor effects from 75 μM ($p < 0.01$). At 75 μM, VOsil and VOchrys were more deleterious than cisplatin (74, 76, vs 98 % survival), whereas at 100 μM, the differences were 32, 56 vs 88 % surviving cells, respectively.

Cytotoxicity studies

To obtain deeper insight into the antiproliferative effects of the complexes, the cytotoxicity of VOchrys and VOsil toward relevant organelles of the cells (mitochondria and lysosomes) was investigated through the reduction
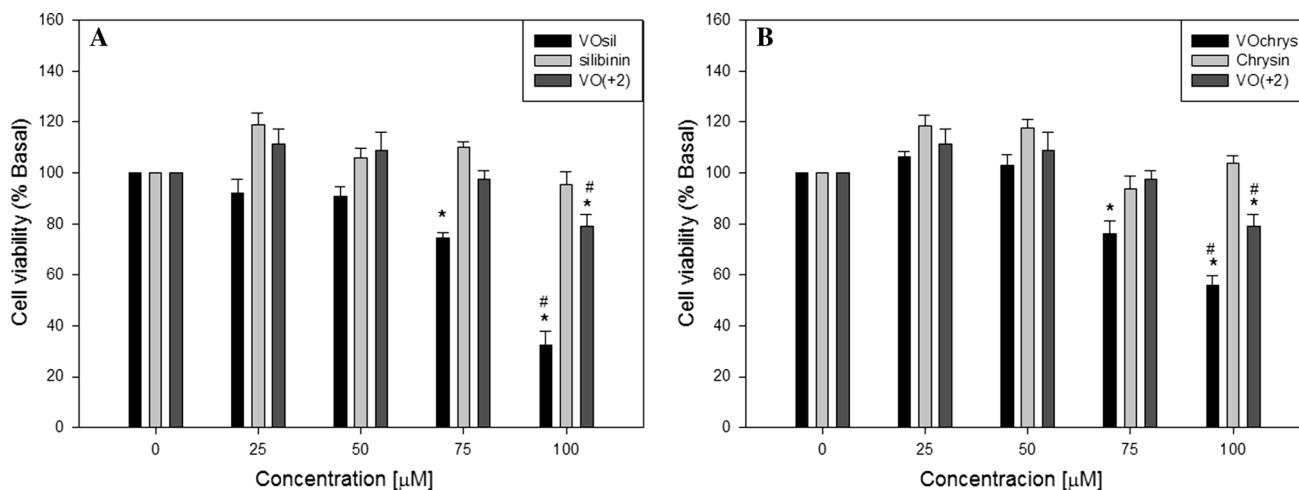
Fig. 2 Effects of VOsil, silibinin and vanadyl cation (**a**) and VOchrys, chrysin and vanadyl cation (**b**) on HT-29 human cell line viability evaluated by crystal violet assay. Cells were incubated in serum-free DMEM alone (control) or with different concentrations of the complexes, free ligands and free metal at 37 °C for 24 h. The results are expressed as the percentage of the basal level and represent the mean ± SEM ($n = 18$). *Significant difference in comparison with the basal level ($p < 0.01$). #Significant differences between the complex and the free metal ($p < 0.01$)
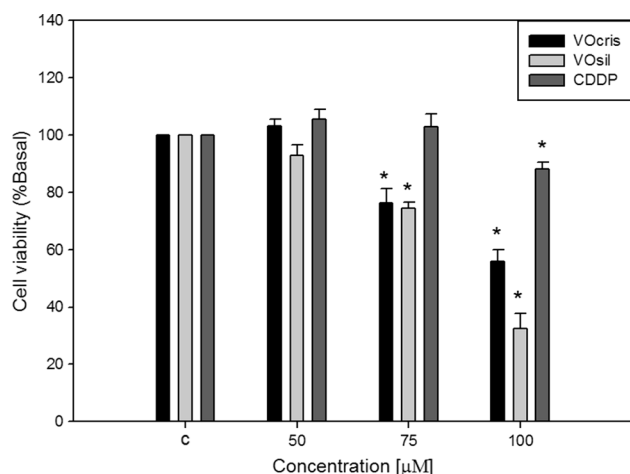
Fig. 3 Effects of VOsil, VOcrys and cisplatin (CDDP) on HT-29 cells evaluated by crystal violet assay. Cells were incubated in serum-free DMEM alone (control) or with different concentrations of the complexes at 37 °C for 24 h. The results are expressed as the percentage of the basal level and represent the mean ± SEM ($n = 18$). *Significant difference in comparison with the basal level ($p < 0.01$)

of MTT assay and the neutral red (NR) uptake assay, respectively.

Alteration in the energetic metabolism of the HT-29 cells was determined by the MTT assay. This technique measures the ability of the mitochondrial succinic dehydrogenases to reduce the methyl tetrazolium salt [31].

On the other hand, the NR technique is used to measure the growth of a population of cultured cells: viable cells take up the NR dye and transport it to the lysosomes [32].
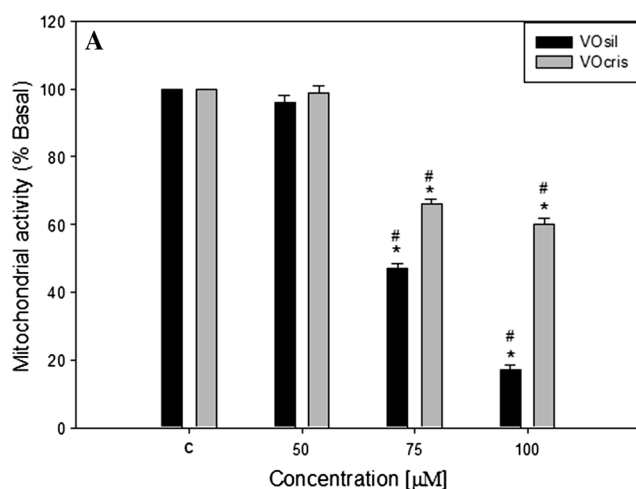
The metabolically active lysosomes display the capacity of taking up the NR dye.

Figure 4a shows the effects of both complexes on the mitochondrial metabolism of colorectal adenocarcinoma cells. A concentration-related inhibition was observed from 75 to 100 μM with statistically significant differences against the control condition ($p < 0.01$). Moreover, VOsil produced stronger cytotoxic effects than VOchrys.

Besides, Fig. 4b shows the effects of VOsil/VOchrys on lysosomal activity of HT-29 cells. The data presented herein show a cytotoxic effect of the complexes in a concentration-dependent manner from 75 to 100 μM ($p < 0.01$). These results are in agreement with the effect of VOsil and VOchrys on mitochondrial activity.

Mechanism of action

The putative cell death mechanisms triggered by VOchrys/VOsil were investigated through the determination of the GSH/GSSG redox couple, apoptosis and cell cycle arrest. Moreover, an exhaustive study of the inhibition of topoisomerase IB activity and the NF-kB activation was also performed.

Cellular redox status

For a better understanding of the possible mechanism involved in the cytotoxicity of both complexes in HT-29 cells, we evaluated the effect of VOchrys and VOsil on the ratio of GSH to GSSG. GSH is one of the major reducing agents in mammalian cells. This thiol acts by sequestering
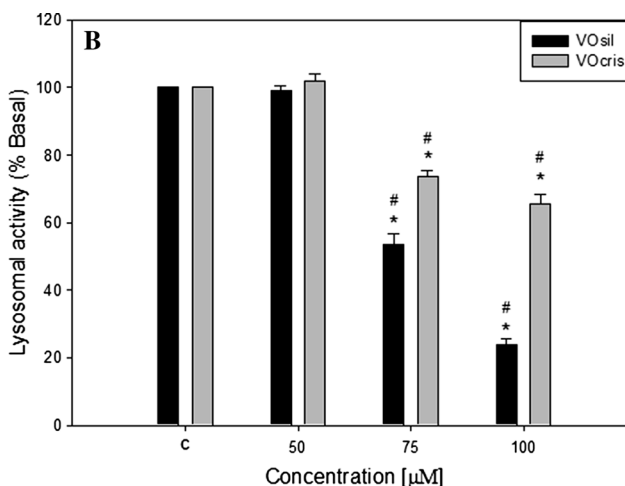
Fig. 4 a Evaluation of the mitochondrial succinate dehydrogenase activity by the MTT assay in HT-29 cells in culture. HT-29 cells were incubated with different concentrations of the VOsil and VOchrys at 37 °C for 24 h. After incubation, cell viability was determined by the MTT assay. Results are expressed as % basal and represent the mean ± SEM, $n = 18$, *$p < 0.01$. **b** NR uptake by HT-29 colon adenocarcinoma cells in culture. Tumor cells were incubated with different concentrations of VOsil and VOchrys for 24 h at 37 °C. After incubation, cell viability was determined by the uptake of NR. The dye taken up by the cells was extracted and the absorbance read at 540 nm. Results are expressed as % basal and represent the mean ± SEM, $n = 18$, *$p < 0.01$
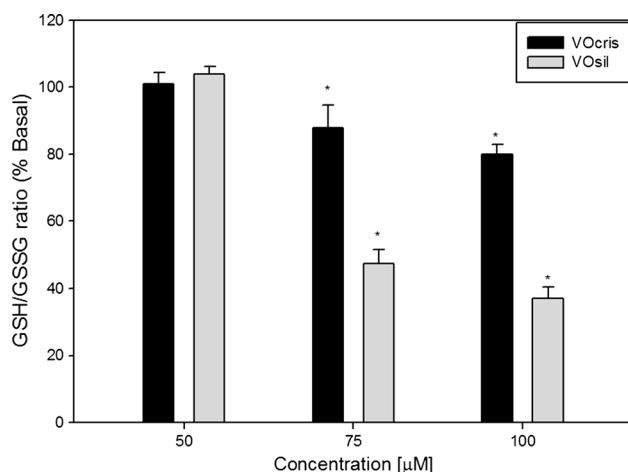
Fig. 5 GSH/GSSG ratio in HT-29 cells, incubated with 50, 75 and 100 µM of VOsil and VOchrys. Results are expressed as mean ± SEM of three independent experiments $n = 12$. *Significant differences vs. basal ($p < 0.01$)

Table 1 E_{hc} (mV) values calculated using the Nernst´s equation at 25 °C, pH 7.4

E_{hc} (mV)	VOchrys	VOsil
Control	249 ± 4	243 ± 5
75 µM	229 ± 6	193 ± 6
100 µM	221 ± 5	177 ± 3

free radicals and regulating the redox status by means of the GSH/GSSG couple [37].

Figure 5 shows the effects of VOsil/VOchrys on GSH/GSSG levels in HT-29 cells. As it can be seen, VOsil and VOchrys caused a decrease in the ratio of GSH to GSSG in HT-29 cells in the range of 75–100 µM ($p < 0.01$). At 75 µM, VOsil was more deleterious than VOchrys (47 vs 87 % of GSH/GSSG ratio), whereas at 100 µM, the differences were 37 vs 80 % of GSH/GSSG, respectively.

On the other hand, the redox state of a redox couple is defined by the half-cell reduction potential and the reducing capacity of that couple.

$$GSSG + 2H^+ + 2e^- = 2GSH.$$

Thus, the Nernst´s equation for the reduction potential of the GSSG/2GSH half-cell will have the form:

$$E_{hc} = -264 - (59.1/2)\log\left([GSH]^2/[GSSG]\right) \text{ mV at } 25°C, \text{ pH } 7.4.$$

Table 1 shows the change in cellular redox potential. As it can be seen, the values of reduction potential decreased from 249 ± 4 to 229 ± 6 and 221 ± 56 after the treatment with 75 and 100 µM of VOchrys, respectively. Besides, in accordance with the GSH/GSSG ratio results, the values of

E_{hc} highly diminished with the VOsil treatment. The values for the basal condition, and for 75 and 100 µM VOsil treatment are 243 ± 5, 193 ± 6 and 177 ± 3, respectively.

These results are in agreement with the effect of both complexes on the GSH/GSSG ratio and HT-29 cell viability.

Cell cycle analysis and DNA fragmentation

Cells go through the cell cycle in several well-controlled phases [38]. The entry into each phase of the cell cycle is regulated by different checkpoints. One issue emerging from drug discovery is to develop therapeutic agents that target the checkpoints responsible for the control of cell cycle progression. Endonucleases activated during apoptosis target at internucleosomal DNA sections and cause extensive DNA fragmentation [39].

Apoptotic cells have deficient DNA content, and when stained with a DNA-specific fluorochrome (propidium iodide), they can be recognized by flow cytometry as cells with less DNA than G1 cells, known as the ''sub-G1'' peak in the DNA content frequency histograms [40, 41].

Cell cycle arrest and the progression of apoptosis as a function of the incubation time were analyzed by flow cytometry. When the cells were treated with 100 µM of VOchrys, many changes were observed in the cell cycle distribution in a time-dependent manner. With 100 µM of the compound, cell cycle arrest in G2/M phase was seen after 24 h of incubation (Fig. 6). These phase still showed a significant increase after 48 h of incubation with the complex ($p < 0.01$). Besides, it should be noted that under these experimental conditions, no subG1 peak was detected (no DNA degradation). On the other hand, when using 100 µM of VOsil, the cells were directly conveyed to apoptosis after 24 and 48 h of treatment showing a significant increase in the sub-G1 peak (35 % apoptotic cells vs 3 % control).

Apoptosis

Apoptosis is a physiological process of cell death enhanced in the presence of harmful agents. Apoptosis produces various modifications in the cell structure, mainly at the cellular membrane level. Cell death may be triggered by an extrinsic pathway mediated by receptors on the surface of the cells or can be produced by endoplasmic reticulum or mitochondrial stress (intrinsic pathway). Consequently, a genetic program that leads to cell death is activated. Apoptosis is characterized by some morphological changes in the cytoplasm and the nucleus. Because of this, apoptosis can be assessed by using several characteristic features of programmed cell death. One of the first alterations that can be defined is the externalization of phosphatidylserine at the outer plasma membrane leaflet (early apoptosis). Other
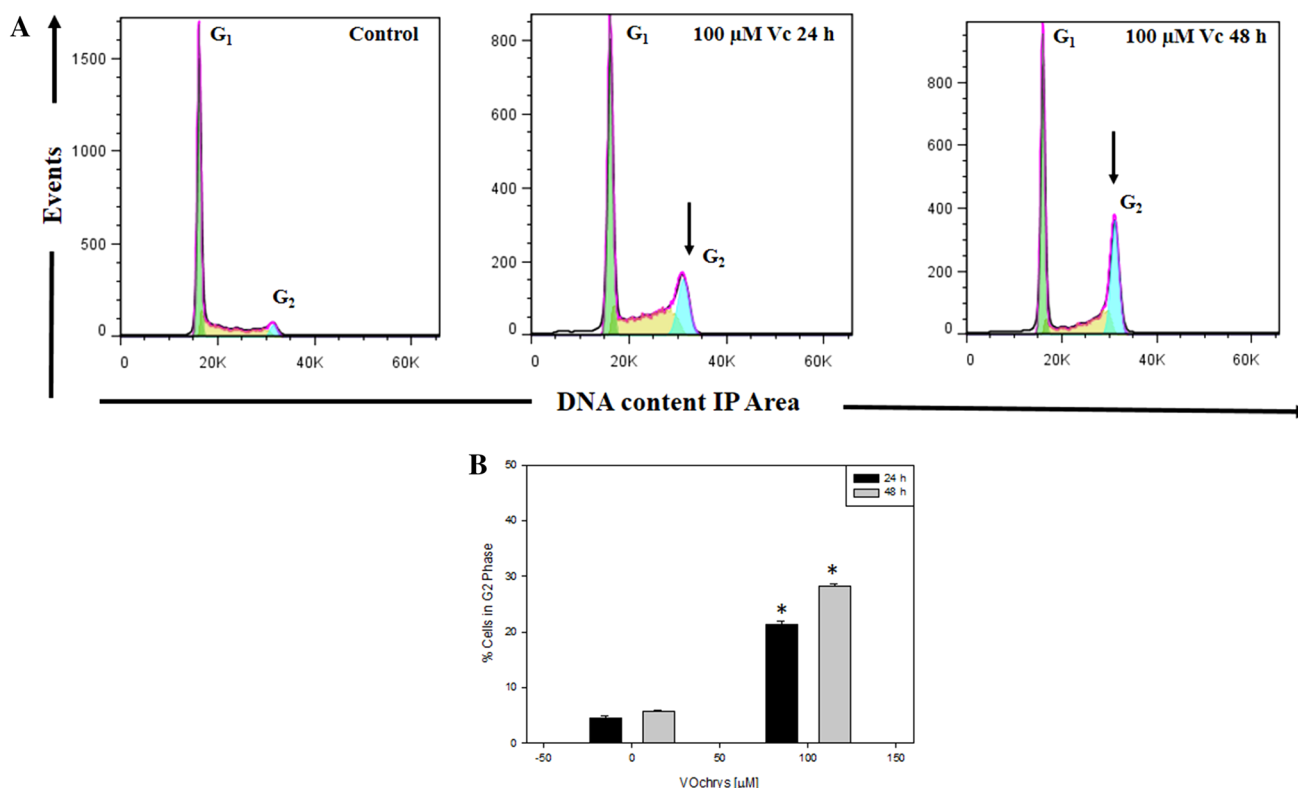
Fig. 6 Effect of VOchrys on cell cycle arrest and DNA fragmentation. **a** Effects of VOchrys on cell cycle arrest (G2 phase). HT-29 cells were treated with 0 (control) and 100 µM of VOchrys at 37 °C during 24 and 48 h. **b** *Graphical bars* show the percentage of G2 phase cells. Results are expressed as the mean ± SEM, $n = 9$. *Significant differences vs.control ($p < 0.05$). Plots are representative of three independent experiments

important features of apoptosis are the activation of the caspase pathway and DNA fragmentation.

Effects of VOsil on phosphatidylserine externalization

Independently of the cell type and the nature of the injuring agent, the externalization of phosphatidylserine is always present in the earlier apoptotic events. Annexin V–FITC is a fluorescent probe with high affinity for phosphatidylserine, allowing its determination by fluorescence assays. Moreover, propidium iodide (PI) is a probe with high affinity for DNA. When the plasmatic membrane is not altered, PI cannot enter the cells but as apoptosis progresses the cellular membrane is damaged and PI enters the cells. These occur in the late steps of apoptosis events.

To obtain deeper insight into the apoptosis induced by both complexes, we tested 100 µM of each complex and two incubation times (6 and 24 h).

Table 2 and Fig. 7 display the quantification of early and late stages of apoptosis obtained by flow cytometry in HT-29 cells.

Table 2 shows that after 6 h of incubation, the basal condition showed 5 % of early apoptotic cells annexin V(+)

Table 2 Level of early and late apoptosis in HT-29 cells

Complex [µM]	Annexin V(+)/PI(−)		Annexin V(+)/PI(+)	
	6 h	24 h	6 h	24 h
Control	5 ± 0.5	5 ± 1	2 ± 0.2	3 ± 0.5
100 µM VOchrys	6 ± 0.5	6 ± 1	3 ± 0.5	2.5 ± 0.5
100 µM VOsil	12 ± 1*	6 ± 1	33 ± 2*	56 ± 5*

* Significant difference in comparison with the basal level ($p < 0.01$)

and 2 % of late apoptotic cells annexin V(+)/PI(+). After 6 h of treatment, VOsil increased the levels of early apoptotic cells and late apoptotic cells (12 and 33 %, respectively), while VOchrys did not produce changes in these cells populations. On the other hand, after 24 h of treatment, VOsil resulted in approximately 56 % of late apoptotic cells, with a statistically significant difference with the control and produced a striking increase in this fraction of apoptotic cells (see Fig. 7).

As can be seen, the percentages of early and late apoptotic cells increased only for incubation with VOsil. These results are in accordance with the viability assays, GSH
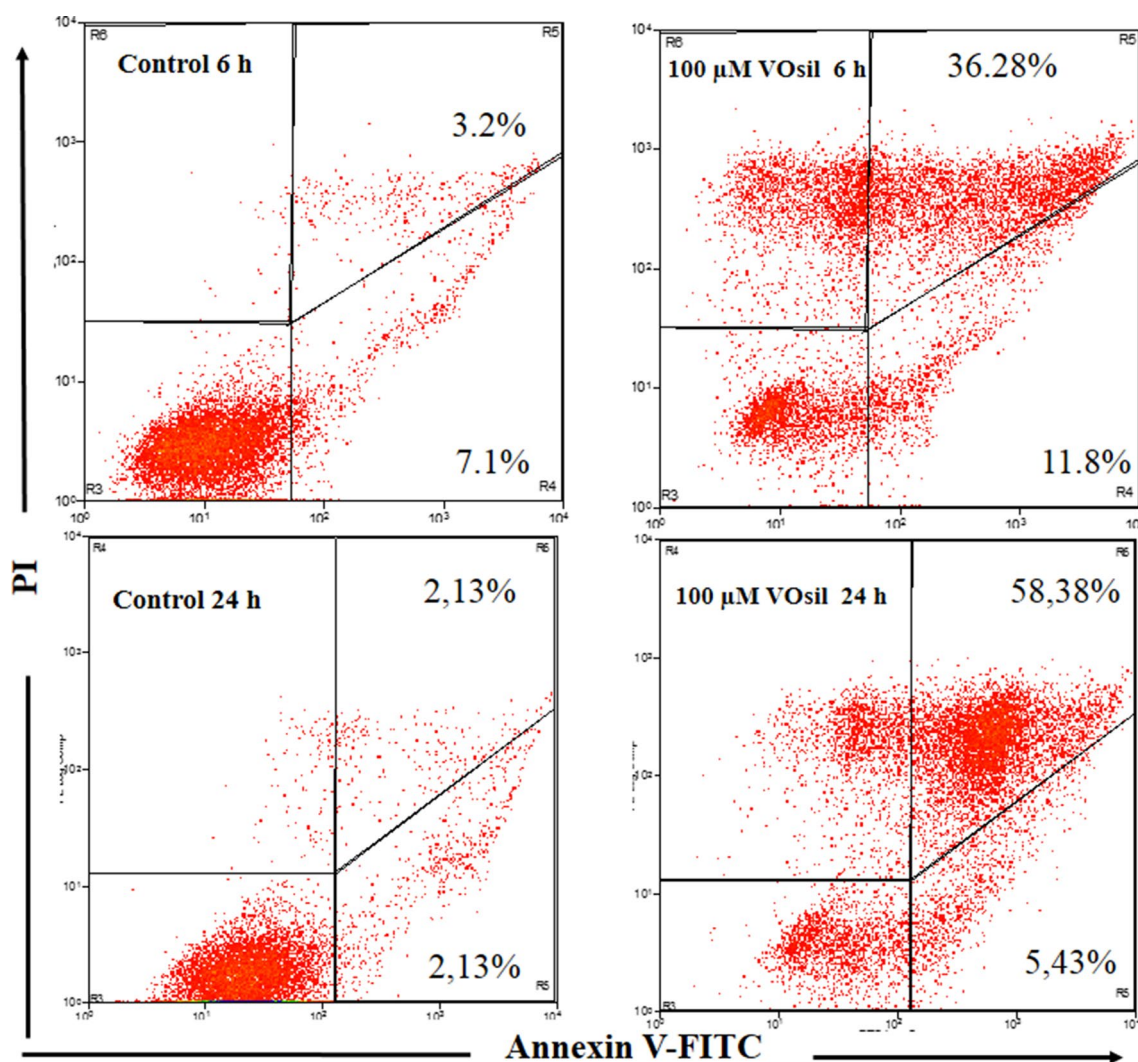
Fig. 7 Effect of VOsil on apoptosis assessed by flow cytometry using Annexin V-FITC/PI staining. HT-29 cells were treated with 0 (control) and 100 μM of the complex at 37 °C during 6 and 24 h. Plots are representative of three independent experiments. Numbers in R5 quadrant indicate the Annexin V(+) cells

levels and cell cycle distribution, confirming the deleterious action of VOsil on HT-29 cells.

Caspase 3 activation

Caspases (cysteine-requiring aspartate proteases) are a family of proteases that mediate cell death and these enzymes are very important to the process of apoptosis. Caspase 3 is one of the critical members of this family since it is an effector caspase that cleaves most of the caspase-related substrates involved in apoptosis regulation [42, 43]. It plays a central role mediating nuclear apoptosis, including chromatin condensation and DNA fragmentation as well as cell blebbing [44]. Figure 8 shows the effects of VOsil on caspase 3 activation. In this figure, it can be seen that after 6 h of incubation of the cells with VOsil and VOchrys, caspase

3 is activated only in the presence of 100 μM of VOsil ($p < 0.01$), demonstrating that the apoptotic effect of VOsil is in agreement with the annexin V/PI assay. The activation of caspase 3 is a very good marker to confirm the annexin V results for the detection of apoptosis.

Effect of VOchrys and VOsil on NF-kB activation

NF-κB (nuclear factor kappa-light-chain-enhancer of activated B cells) is a protein complex that controls transcription of DNA. The NF-kB is widely used by eukaryotic cells as a genetic regulator of cell proliferation and cell survival. Therefore, many types of human tumors show an activation of the NF-kB to prevent death and protect the cell against the apoptosis. Defects in NF-kB produce an increased susceptibility to apoptosis leading to an increase in cell death

Fig. 8 Effect of VOsil on caspase 3 activation. Activity of caspase 3 was determined with the caspase 3-specific antibody coupled FITC. HT-29 cells were treated with VOsil at 0 (control) and 100 μM at 37 °C for 6 h and were then harvested and analyzed by flow cytometry. The results are expressed as the mean ± SEM of three independent experiments ($n = 9$). *Significant differences versus the control ($p < 0.01$)
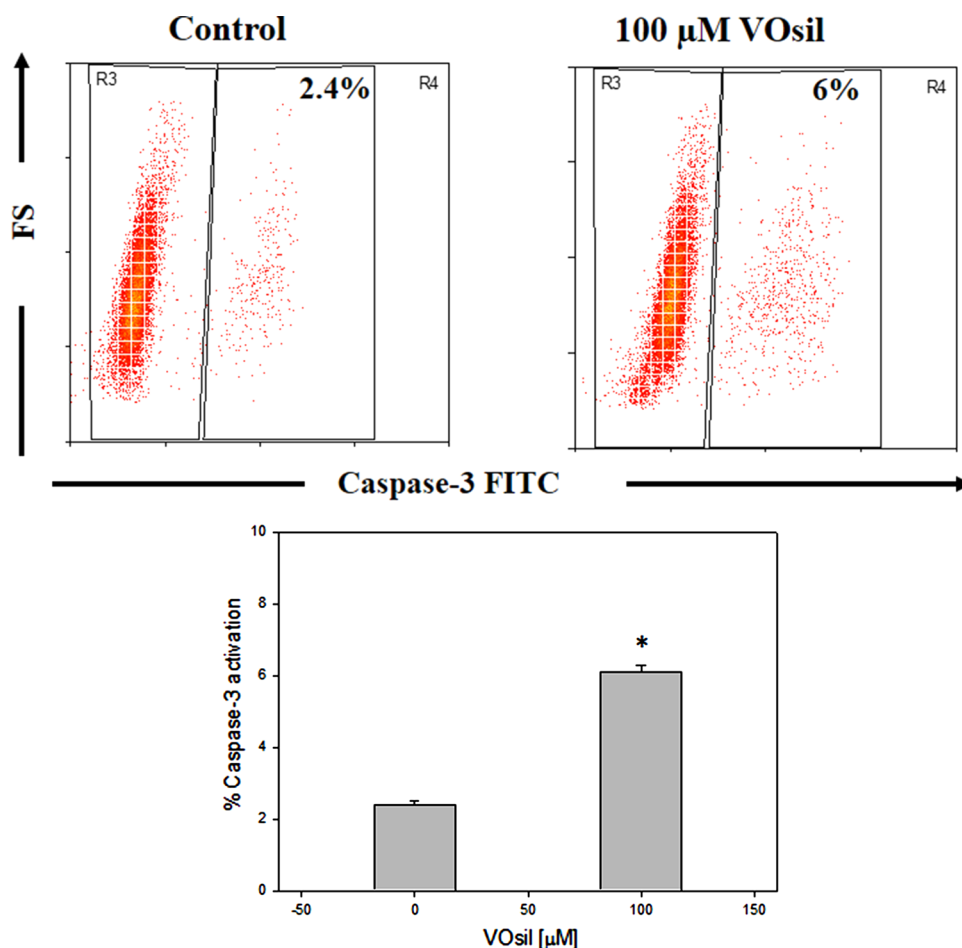
due to the fact that NF-kB regulates anti-apoptotic genes (especially TRAF1 and TRAF2), that controls the caspases' enzymatic activity [45]. The inactivation of NF-kB may cause that the tumoral cells cease to proliferate, die, or are more sensitive to the action of anticancer agents. Therefore, NF-kB is an important target to be studied in cancer therapy [46]. Furthermore, NF-kB plays a key role in the inflammatory response that is why the inhibition of NF-kB signaling pathway has a strong interest in cancer therapies and inflammatory diseases [47].

For a better understanding of the role of the NF-kB inhibition in cell death, we tested two concentrations (25 and 50 μM) of both complexes in presence of the tumor necrosis factor (TNF-α), the activator of this signaling pathway, using HT-29 colorectal adenocarcinoma line transfected with the gene NFκBhrGFP.

As it can be seen in Fig. 9, VOchrys did not show effects in the inhibition of NF-kB pathway. On the contrary, after VOsil treatment (50 μM), the activation of NF-kB pathway by TNF-α is inhibited by the complex. Figure 9 shows that when NF-kB pathway was activated by TNF-α, 49 % of activated cells can be seen, this value decreases to 27 % with a pre-treatment of 50 μM of VOsil, demonstrating the

inhibitory effect of the complex in the NF-kB pathway. This behavior would be closely related to the pro-apoptotic effects generated by VOsil in HT-29 cells. As mentioned above, there are numerous reports linking NF-kB activation as a way to escape from apoptosis and activation of cell proliferation [48]. VOsil would be involved in the inhibition of this pathway increasing the sensitivity of cells to apoptosis which in turn is generated by the same compound, as we have shown previously. These results are consistent with all those obtained up here, demonstrating that the deleterious and pro-apoptotic effect is stronger in Vosil than VOchrys.

Effect of VOchrys and VOsil on topoisomerase IB activity and relaxation

Topoisomerases are enzymes that control the topological state of DNA through the breaking and rejoining of DNA strands. Currently, there are two classes of topoisomerases: type I enzymes, which act by transiently nicking one of the two DNA strands, and type II enzymes which nick both DNA strands and whose activity is dependent on the presence of ATP. Topoisomerases are involved in different
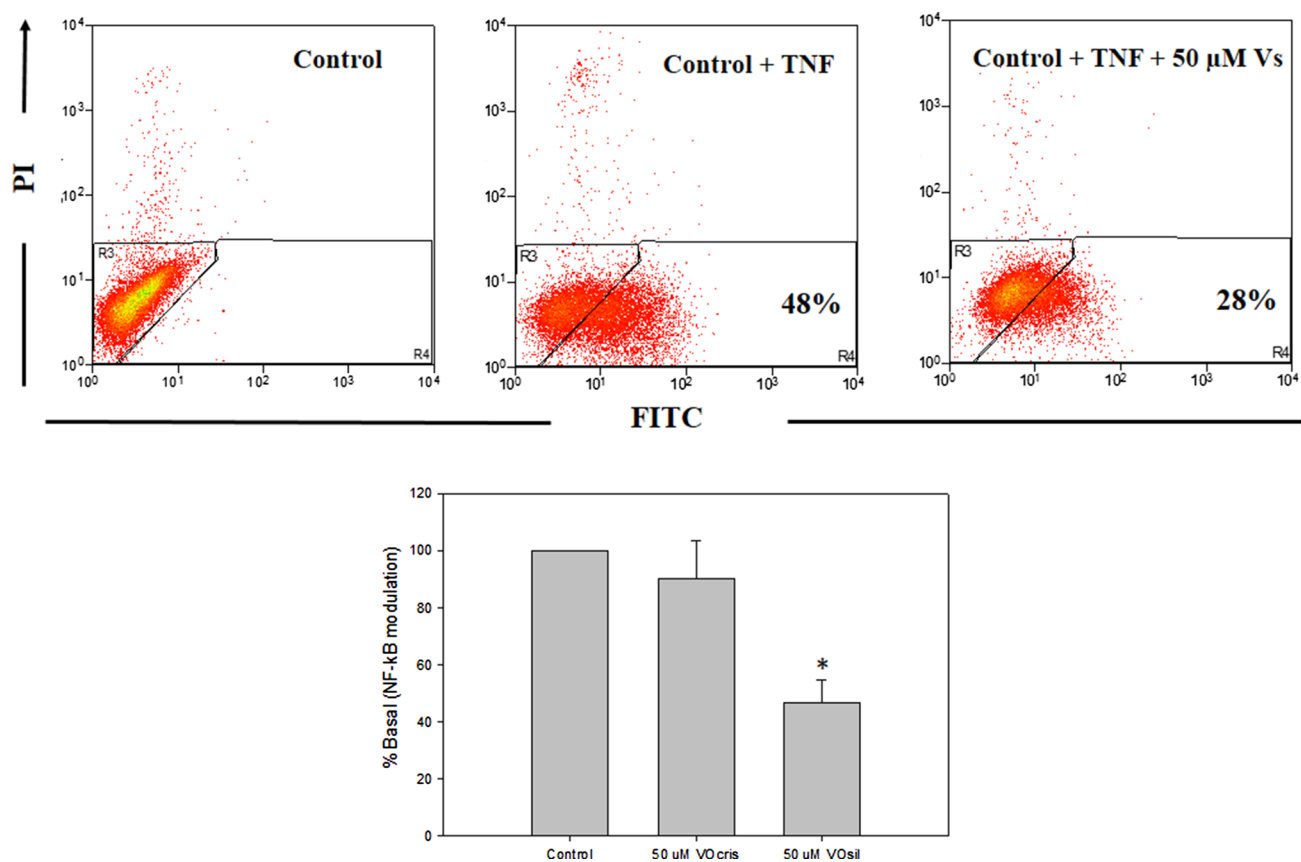
Fig. 9 Effect of VOsil on NF-kB activation by TNF-α. NF-kB activation was determined using HT-29 colorectal adenocarcinoma line transfected with the gene NFκBhrGFP (HT-29-NF-κB-hrGFP). This cells were pretreated with VOsil and VOchrys 0 (control) 25 and 50 μM during 2 h before stimulation with 3ng/mL of TNF-α for 18 h. Then the cells were then harvested and analyzed by flow cytometry. The results are expressed as the mean ± SEM of three independent experiments ($n = 9$). *Significant differences versus the control ($p < 0.01$)

cellular processes such as DNA replication, transcription, recombination, integration and chromosomal segregation [49, 50]. In the last years, many reports suggest that topoisomerases are targets of several antitumor agents since these compounds reduce the topoisomerase activity acting through different mechanisms [51, 52]. Figure 10 shows the effects of VOsil on the human topoisomerase IB relaxation activity. From this figure, it can be seen that VOsil has an inhibitory effect on the topoisomerase IB relaxation activity in a dose-dependent manner from 75 to 300 μM (Fig. 10a, lanes 7–11), a full inhibition being achieved at 100 μM. Figure 10b shows that the enzyme fully relaxes the substrate in the absence of the compound (lanes 2–5), and partially relaxes the substrate in presence of 55 μM of VOsil (lanes 6–9) but the DNA relaxation is inhibited if the enzyme is pre-incubated with the vanadium complex VOsil (lanes 10–13). Nevertheless, as it can be seen from Fig. 10b (lanes 12–13) that the inhibition is incomplete indicating that the inhibitory effect of the vanadium compound is reversible. On the other hand, VOchrys did not show effects on topoisomerase IB activity.

Analysis of cleavage and religation kinetics

The cleavage and the religation reactions have been carried out in separate experiments to clarify if the vanadium compound inhibits the relaxation reaction affecting one of the two processes or both of them. The cleavage kinetics has been followed by reacting an excess of topoisomerase I with the suicide substrate (Fig. 11a), in the absence and the presence of VOsil. Figure 11b shows the PAGE analysis of the reaction products, where the band corresponding to the cleaved DNA fragment is indicated as CL1. The cleavage kinetics is very fast in the control condition (absence of the compound), while it is strongly reduced in the presence of 150 μM of VOsil. Besides, the pre-incubation effects with the enzyme before the substrate addition increased the inhibitory effect of VOsil but this effect is reversible (Fig. 11b, lanes 14–19).

The religation kinetics has been performed incubating the suicide cleavage substrate with an excess of native enzyme for 30 min to produce the cleaved complex,
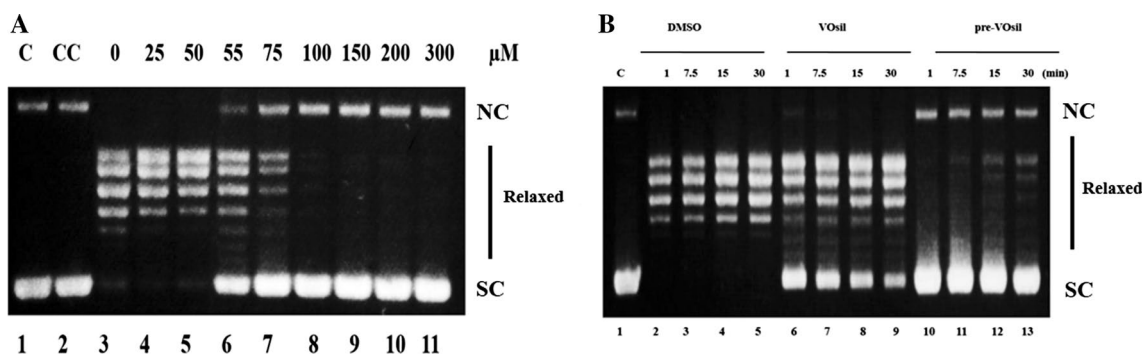
Fig. 10 a Relaxation of negative supercoiled plasmid DNA by topoisomerase IB in the presence of increasing concentration of VOsil (*lanes 3–11*). The reaction product was resolved in an agarose gel and visualized with ethidium bromide. *Lane* 1 no protein added and *lane* 19 control reaction with DNA and DMSO without VOsil. *NC* nicked circular plasmid DNA, *SC* supercoiled plasmid DNA. **b** Relaxation of negative supercoiled plasmid DNA in a time course experiment with DMSO (*lanes 2–5*), in the presence of 55 µM VOsil (*lanes 6–9*), after pre-incubation of 55 µM VOsil with the enzyme for 5 min at 37 °C (*lanes 10–13*). *Lane* 1 no protein added

Fig. 11 a The CL14/CP25 suicide substrate used to measure the cleavage kinetics of the enzyme. The preferred topoisomerase I binding site is indicated by an asterisk. **b** Cleavage kinetics of topoisomerase IB alone (*lanes 2–7*), in the presence of 150 µM VOsil (*lanes 8–13*), and after 5 min pre-incubation of 150 µM VOsil with the enzyme (*lanes 14–19*). *Lane* 1 no protein added. CL1 represents the DNA fragment cleaved at the preferred enzyme site. **c** The suicide substrate CL14/CP25 and the R11 complementary oligonucleotide used to measure the religation kinetics of the enzyme. **d** Urea-polyacrylamide gel electrophoretic analysis of the religation kinetics of topoisomerase IB in the absence (*lanes 2–9*) or in the presence of 150 µM VOsil (*lanes 10–17*). *Lane* 1 represents the substrate alone
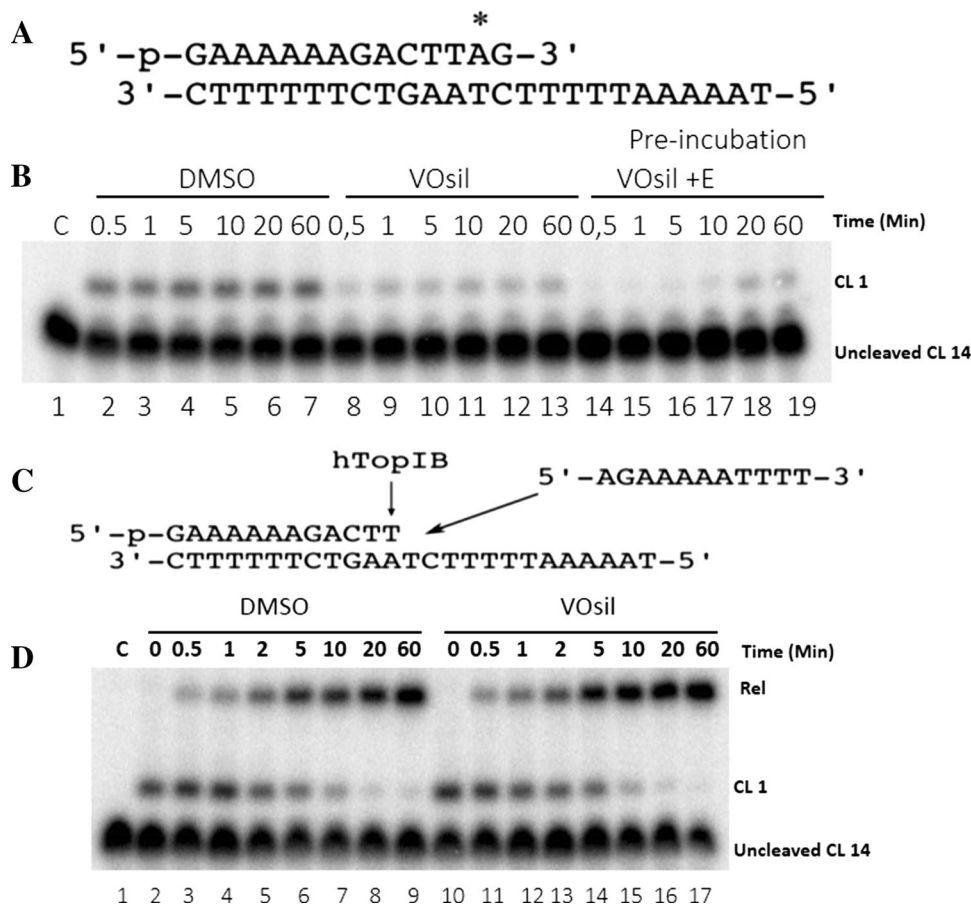
followed by subsequent addition of 200-fold molar excess of the R11 complementary oligonucleotide in the presence of DMSO and VOsil. As it can be seen from Fig. 11d, the religation rate is the same in the presence or in the absence of VOsil (Fig. 11d, lanes 10–17) concluding that the compound did not show inhibitory effects in the religation reaction.

Binding analysis by EMSA

The inactive Y723F human topoisomerase IB mutant was incubated with the radiolabelled CL25/CP25 DNA substrate in presence of DMSO, 150 µM VOsil or pre-incubated with 150 µM VOsil for 5 min (Fig. 12, lanes 3–5). In the absence of the protein and the protein with 1 % of
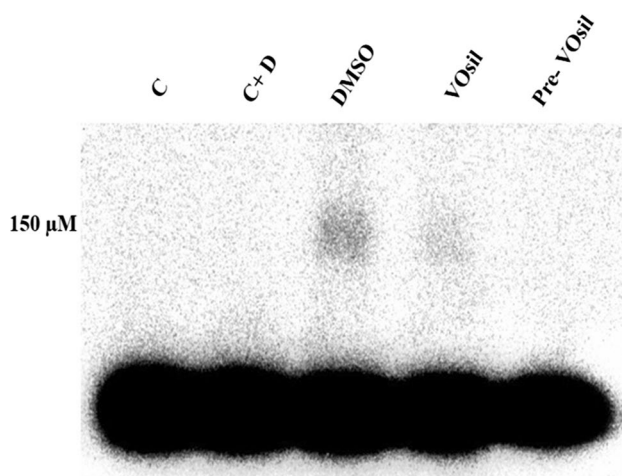
Fig. 12 Electrophoretic mobility shift assay of the [γ 32P] radiolabelled substrate CL25/CP25 alone (*lane* 1), in the presence of DMSO (*lane* 2), of inactive mutant Y723F enzyme (*lane* 3), of the mutant and 150 μM VOsil (*lane* 4), after 5 min pre-incubation of 150 μM VOsil with the mutant (*lane* 5)

DMSO, no DNA shift was observed (Fig. 12, lane 1–2). In the presence of the mutant, a tiny slowly migrating band, corresponding to a DNA-topoisomerase IB complex, is formed (Fig. 12, lane 3). The band is not observed when VOsil (150 μM) is present (Fig. 12, lane 4) or is pre-incubated with the enzyme (Fig. 12, lane 5). These results demonstrate that VOsil acts by preventing the topoisomerase IB–DNA complex formation.

Discussion

Vanadium complexes are a group of drugs with potential pharmacological effects [7, 53]. Recently, there has been increasing interest in the antitumor effects of vanadium derivatives [7, 54]. It was previously demonstrated that vanadium compounds cause a reduction of tumor growth both in vitro and in vivo systems [9, 55]. As part of a research project, we have addressed the investigation of the anticancer effects of two oxidovanadium(IV) complexes with chrysin (VOchrys) and silibinin (VOsil) against human colon adenocarcinoma cells. Colon cancer is one of the most common malignancies with high prevalence and low 5-year survival. It is a heterogeneous disease with a complex, genetic and biochemical background where different intracellular signaling pathways are frequently deregulated (Ras, p53, etc.). For this reason, we chose the HT-29 cell line derived from a human colorectal adenocarcinoma because according to the literature, it is a very interesting model and one of the most used cell lines for colon cancer research [56].

In this work, we have investigated the cytotoxic effects of VOchrys and VOsil and we have elucidated the putative mechanism of action underlying their effects.

Our results demonstrated the beneficial effect of complexation on the antitumor action as shown in Fig. 2. VOsil and VOchrys caused the main deleterious action in the tumor cells in comparison with the vanadyl cation and the free flavonoids. These results were similar to those obtained with these oxidovanadium (IV) complexes against osteosarcoma cells, for which the beneficial effects of metal coordination were also observed [27, 28]. On the other hand, the anticancer effects of VOsil and VOchrys were compared with those of the reference antitumor drug cisplatin, and our results showed very good correlation between these compounds, indicating that VOsil and VOchrys may be placed in the category of non-platinum antitumor drugs. In this sense, different vanadium complexes with thiosemicarbazones derivatives showed anticancer effects against HT-29 cells only at very high concentration (150–280 μM) in comparison with the low concentration tested (75–100 μM) for VOsil and VOchrys [57]. These results show the importance of antitumor properties of VOsil and VOchrys in comparison with other vanadium complexes that show anticancer activity. The lower range of concentrations where these two compounds exert anticancer effects is an important feature for compounds to be studied as potential anticancer drugs. In this sense, the deleterious effects of VOsil and VOchrys have been previously tested by our group on the peripheral blood mononuclear cell (PMBC) as a normal control. The results showed no deleterious actions for VOchrys in the range of concentrations (25–100 μM) μM and only a minimum effect at 100 μM of VOsil against PMBC [28].

Taken together, these results indicate that VOsil and VOchrys are interesting candidates for potential antitumor uses.

Some of the relevant features for anticancer drugs is the stability under physiological conditions and the characterization of the active species [58]. The two compounds investigated herein have shown a very good stability at physiological pH as it has been demonstrated by UV–VIS and EPR spectroscopy [11, 12].

On the other hand, from the EPR data, Sanna and col. have recently described that chrysin and silibinin ligands form penta-coordinated species with (CO, O–) or "acetylacetone-like" coordination (see Supplementary Data, Fig. 1) [59, 60]. This type of behavior has also been reported for other VO–flavonoid complexes such us apigenin, galangin and kaempferol [59]. These acetylacetone-like species display low interaction with the proteins and different blood molecules keeping their structure because they have good stability under physiological conditions [61]. The biological effects of vanadium compounds are highly influenced by the oxidation states of the metal, the nature of the ligands, the coordination sphere and the environmental conditions [62].

In an attempt to elucidate the mechanism of action involved in the antiproliferative effects of VOsil, we studied GSH levels (the main defense antioxidant agent in mammalian cells), topoisomerase IB activity and the inhibition of NF-kB via. In addition, a detailed study of the cell cycle arrest and apoptosis was also performed. Our results showed that VOsil and VOchrys impaired the GSH/GSSG ratio from 75 to 100 μM. Besides, it is generally known that the GSH-related thiols participate in many important biological processes, including the protection of cell membranes against oxidative damage. Overall, it can be assumed that the free radicals decrease the concentration of important cellular compounds and impair the antioxidant system, making cells more vulnerable to oxidative damage. We have previously reported similar results for these and others oxidovanadium(IV) complexes in osteoblast-like cells in culture [27, 28, 63]. Besides, vanadium(V) derivatives diminished the GSH levels in diabetic rat liver and the GSH levels are related to the neoplastic transformation and toxicity in mouse embryo cells [64, 65]. Moreover, vanadium(V) species depleted GSH level in whole blood components including plasma and cytosolic fraction showing the importance of GSH as biomarker of toxicity [66].

To better understand the possible mechanism involved in the cytotoxicity, an exhaustive study of apoptosis and cell cycle analysis were also performed.

Apoptosis is considered a physiological mechanism of cell death, inherent to cellular development, which is triggered by different endogenous or exogenous factors [67].

This process is accompanied by a characteristic of morphological changes on the cytoplasm and the nucleus of the cells. Independent of the cellular type and the nature of the trigger agent, the externalization of PS is always present in the earlier apoptotic events.

Our flow cytometry results showed that the percentages of apoptotic and apoptotic/necrotic cells increased with the exposure time for VOsil while did not show any effect after treatment with VOchrys. Besides, VOsil induced the activation of caspase-3, while VOchrys did not show effects. These results are in accordance with the viability assays, confirming the deleterious actions of VOsil in HT-29 cell line.

On the other hand, VOchrys produced a cell cycle arrest in G_2/M phase after 24 and 48 h while VOsil conveyed the cells directly to death through apoptosis. Clearly, two mechanisms of action seem to be involved in the decrease of tumor cell survival by vanadium–flavonoid compounds. These mechanisms are dependent on the compound: VOchrys only caused the arrest of the cell cycle at G_2/M phase while VOsil disrupted cell survival sending the tumor cells directly to programmed cell death.

Previous results also showed that other vanadium compounds caused a cell cycle arrest and increase the number of apoptotic cells. In fact, simple inorganic vanadium(IV) and vanadium(V) compounds ($VOSO_4$, $NaVO_3$, and vanadium pentoxide) induced apoptosis in different cancer cell lines [68–70].

Recent articles have shown that in isolated rat liver hepatocytes as well as in an N27 dopaminergic neuronal cell model, vanadium induced cytotoxicity through apoptosis and an increase in the levels of caspase 3 [71, 72]. Moreover, orthovanadate induced caspase-dependent apoptosis in thyroid cancer cells and inhibited growth through apoptosis in human hepatocellular carcinoma [68, 73]. Besides, NH_4VO_3 caused cell cycle arrest and apoptosis in a dose-dependent manner in human breast cancer cells [74] and vanadyl bisacetylacetonate complex caused a cell cycle arrest in G1 phase in a dose- and time-dependent manner in hepatocarcinoma cells [75].

Aberrant activation of NF-κB is frequently observed in many types of cancers and in inflammatory processes. Therefore, several methods of inhibiting NF-κB signaling have potential therapeutic application in cancer and inflammatory diseases [76].

Recent bibliographic works have highlighted the importance of the linkage between NF-κB, inflammation and cancer, showing the importance of the regulation of the activity of NF-κB in cancer therapy [77].

Research articles show the effects of several agents such us carotenoids and flavonoids derivatives on the activity of NF-κB signaling pathway in cancer cells [78, 79].

Nevertheless, the literature has scarce reports about the action of metal-based drugs on the NF-κB system. Our research shows for the first time the effects of oxidovanadium(IV) complexes with potential therapeutic applications on the NF-κB target. These vanadium compounds demonstrate different activity on this pathway. VOchrys did not cause any inhibitory action while VOsil reduced the activity of NF-κB path showing a good correlation with the cell viability and mechanistic study results.

A possible mechanism of action whereby vanadium compounds may modulate the NF-κB pathway involves the complex I and complex II formation [48]. The membrane-associated complex I comprises TRADD, RIP1 and TRAF2 and is responsible for rapid NF-κB dependent expression of genes encoding antiapoptotic molecules while the cytosolic complex II, consisting of TRADD, RIP1, TRAF2, FADD, caspase-8 and caspase-10, is proapoptotic [80]. After TNF stimulation, rapid assembly of complex I occurs at the TNF receptor, triggering NF-κB activation through recruitment of the IKK complex. After that, a substantial amount of TRADD–RIP1–TRAF2 dissociates from the receptor, binding FADD and caspases in the cytosol to induce programed cell death. It is thought this action that complex II is able to trigger apoptosis only when NF-κB activation is blocked or induces insufficient amounts of antiapoptotic proteins such as XIAP or $FLIP_L$ [48].

Finally, here, we show that VOsil inhibits topoisomerase IB activity using plasmid relaxation assay and the result shows that the inhibitory effect is increased when the complex is pre-incubated with topoisomerase IB before DNA addition. Our results suggest that VOsil is able to interact with the enzyme alone, likely inhibiting the topoisomerase activity. This prompt is confirmed and demonstrate that VOsil acts as a cleavage inhibitor but without affecting the religation rate. Besides, the topoisomerase IB–DNA interaction study demonstrates that VOsil acts by preventing the topoisomerase IB–DNA complex formation. These results suggest that topoisomerase IB may be an important target for antitumor vanadium compounds scarcely investigated at present.

A recent article has shown that a vanadium compound with diaminothiazole inhibited topoisomerase I activity preventing the enzyme–DNA complex formation [81].

Besides, oxindolimine copper(II) and zinc(II) compounds inhibited the relaxation activity of topoisomerase IB using different mechanisms of inhibition since the copper compound does not allow the binding of the enzyme to DNA at variance of zinc complex [82].

Moreover, four new copper(II) complexes containing phosphonium inhibited the topoisomerase I activity from 40 to 160 μM [83].

Conclusion

New vanadium complexes with potential anticancer activity currently require more intensive basic and applied investigation since this knowledge obtained from in vitro studies may allow vanadium compounds to enter the preclinical in vivo phase. On these bases, we have carefully investigated the mechanisms of action underlying the deleterious effects of two complexes of the oxidovanadium(IV) cation with the flavonoids silibinin, VOsil, and chrysin, VOchrys in a human colon adenocarcinoma cell line (HT-29).

We have demonstrated that the complexation of the flavonoids silibinin and chrysin with vanadyl cation improved the antitumor activity of the free ligand and metal in this tumor human model.

VOsil and VOchrys caused cytotoxicity in a concentration-dependent manner. The principal mechanisms of action involved in the antitumor effects of VOchrys were mediated by a decrease of the GSH levels and cell cycle arrest while VOsil employed different mechanisms that include depletion of GSH, apoptosis induction, attenuation of NF-kB pathway and inhibition of topoisomerase IB activity.

This research intends to contribute to the body of knowledge of the chemical and biochemical properties as well as the mechanisms of the cellular and molecular antitumor activity of vanadium-based drugs.

Taken together, our results show that VOsil is the most interesting candidate for potential antitumor uses, and provide new insight into the development of vanadium compounds as potential anticancer agents.

References

1. Jemal A, Bray F, Center MM, Ferlay J, Ward E, Forman D (2011) CA Cancer J Clin 61:69–90
2. Surh YJ (2003) Nat Rev Cancer 3:768–780
3. Nielsen FH (1995) In: Sigel H, Sigel A (eds) Metal ions in biological systems, vanadium and its role in life. Dekker, New York, pp 543–574
4. Srivastava K, Mehdi MZ (2004) Diabet Med 22:2–13
5. Thompson KH, Lichter J, LeBel C, Scaife MC, McNeill JH, Orvig C (2009) J Inorg Biochem 103:554–558
6. Shioda N, Han F, Fukunaga K (2009) Int Rev Neurobiol 85:375–387
7. Evangelou AM (2002) Crit Rev Oncol Hematol 42:249–265
8. Etcheverry SB, Williams PAM (2009) New developments in medicinal chemistry. In: Ortega MP, Gil IC (eds) Medicinal chemistry of copper and vanadium bioactive compounds. Nova, Hauppauge, pp 105–129
9. Barrio DA, Etcheverry SB (2010) Curr Med Chem 17:3632–3642
10. Köpf-Maier P (1987) Naturwissenschaften 74:374–382
11. Naso LG, Ferrer EG, Butenko N, Cavaco I, Lezama L, Rojo T, Etcheverry SB, Williams PA (2011) J Biol Inorg Chem 16:653–668
12. Naso LG, Ferrer EG, Lezama L, Rojo T, Etcheverry SB, Williams PA (2010) J Biol Inorg Chem 15:889–902
13. Beecher GR (2003) J Nutr 133:3248S–3254S
14. Han X, Shen T, Lou H (2007) Int J Mol Sci 8:950–988
15. Gazák R, Walterova D, Kren V (2007) Curr Med Chem 14:315–338
16. Singh RP, Agarwal R (2004) Curr Cancer Drug Targets 4:1–11
17. Hogan FS, Krishnegowda NK, Mikhailova M, Kahlenberg MS (2007) J Surg Res 143:58–65
18. Ge Y, Zhang Y, Chen Y, Li Q, Chen J, Dong Y, Shi W (2011) Int J Mol Sci 12:4861–4871
19. Koc AN, Silici S, Ayangil D, Ferahbas A, Cankay S (2005) Mycoses 48:205–210
20. Sak K (2014) Pharmacogn Rev 8:122–146
21. Yu XM, Phan T, Patel PN, Jaskula-Sztul R, Chen H (2013) Cancer 119:774–781
22. Li X, Wang JN, Huang JM, Xiong XK, Chen MF, Ong CN, Shen HM, Yang XF (2011) Toxicol In Vitro 25:630–635
23. Uivarosi V, Barbuceanu SF, Aldea V, Arama CC, Badea M, Olar R, Marinescu D (2010) Molecules 15:1578–1589

24. Thompson KH, Orvig C (2001) Coord Chem Rev 219:1033–1053
25. Rehder D, Costa Pessoa J, Geraldes CF, Castro MM, Kabanos T, Kiss T, Meier B, Micera G, Pettersson L, Rangel M (2002) J Biol Inorg Chem 7:384–396
26. Mukherjee R, Donnay EG, Radomski MA, Miller C, Redfern DA, Gericke A, Damron DS, Brasch NE (2008) Chem Commun (Camb) 32:3783–3785
27. Leon IE, Di Virgilio AL, Porro V, Muglia CI, Naso LG, William PAM, Bollati Fogolin M, Etcheverry SB (2013) Dalton Trans 42:11868–11880
28. Leon IE, Porro V, Di Virgilio AL, Naso LG, William PAM, Bollati Fogolin M, Etcheverry SB (2014) J Biol Inorg Chem 19:59–74
29. Okajima T, Nakamura K, Zhang H, Ling N, Tanabe T, Yasuda T, Rosenfeld RG (1992) Endocrinology 130:2201–2212
30. Cortizo AM, Etcheverry SB (1995) Mol Cell Biochem 145:97–102
31. Mosmann TT (1983) J Immunol Methods 65:55–63
32. Borenfreund E, Puerner JA (1984) J Tissue Cult Methods 9:7–9
33. Hissin PJ, Hilf R (1976) Anal Biochem 74:214–226
34. Gong J, Traganos F, Darzynkiewicz Z (1994) Anal Biochem 218:314–319
35. Guimarães FS, Andrade LF, Martins ST, Abud AP, Sene RV, Wanderer C, Tiscornia I, Bollati-Fogolín M, Buchi DF, Trindade ES (2010) BMC Cancer 10:113
36. Chillemi G, Fiorani P, Castelli S, Bruselles A, Benedetti P, Desideri A (2005) NucleicAcids Res 33:3339–3350
37. Jones DP, Carlson JL, Mody VC, Cai JY, Lynn MJ, Sternberg P (2000) Free Radic Biol Med 28:625–635
38. Sherr CJ (2000) Cancer Res 60:3695–3698
39. Nagata S (2000) Exp Cell Res 256:12–18
40. Hurley AA (2001) Curr Protoc Cytom 7.2.1–7.2.5
41. Pozarowski P, Grabarek J, Darzynkiewicz Z (2003) Curr Protoc Cytom 25:7.19.1–7.19.33
42. Nicholson DW, Ali A, Thornberry NA, Vaillancourt JP, Ding CK, Gallant M, Gareau Y, Griffin PR, Labelle M, Lazebnik YA (1995) Nature 376:37–43
43. Sakahira H, Enari M, Nagata S (1998) Nature 391:96–99
44. Porter AG, Janicke RU (1999) Cell Death Differ 6:99–104
45. Sheikh MS, Huang Y (2003) Cell Cycle 2:550–552
46. Escárcega RO, Fuentes-Alexandro S, García-Carrasco M, Gatica A, Zamora A (2007) Clin Oncol 19:154–161
47. Sethi G, Sung B, Aggarwal BB (2008) Exp Biol Med 233:21–31
48. Oeckinghaus A, Hayden MS, Ghosh S (2011) Nat Immunol 12:695–708
49. Champoux JJ (2001) Annu NY Rev Biochem 70:369–413
50. Wang JC (1996) Ann Rev Biochem 65:635–692
51. Boege F, Straub T, Kehr A, Bosenberg C, Christiansen K, Anderson A, Jakob F, Kohrle J (1996) J Biol Chem 271:2262–2270
52. Bridewell DJ, Finlay GJ, Baguley BC (1997) Oncol Res 9:535–542
53. Korbecki J, Baranowska-Bosiacka I, Gutowska I, Chlubek D (2012) Acta Biochim Pol 59:195–200
54. Djordjevic C, Wampler GL (1985) J Inorg Biochem 25:51–55
55. Bishayee A, Waghray A, Patel MA, Chatterjee M (2010) Cancer Lett 294:1–12
56. Trainer DL, Kline T, McCabe FL, Faucette LF, Field J, Chaikin M, Anzano M, Rieman D, Hoffstein S, Li DJ (1988) Int J Cancer 41:287–296
57. Lewis NA, Liu F, Seymour L, Magnusen A, Erves TR, Arca JF, Beckford FA, Venkatraman R, González-Sarrías A, Fronczek FR, Vanderveer DG, Seeram NP, Liu A, Jarrett WL, Holder AA (2012) Eur J Inorg Chem 4:664–677
58. Crans DC, Woll KA, Prusinskas K, Johnson MD, Norkus E (2013) Inorg Chem 52:12262–12275
59. Sanna D, Ugone V, Lubinu G, Micera G, Garribba E (2014) J Inorg Biochem 140:173–184
60. Crans DC, Khan AR, Mahroof-Tahir M, Mondal S, Miller SM, la Cour A, Anderson OP, Jakusch T, Kiss T (2001) J Chem Soc Dalton Trans 3337–3345
61. Sanna D, Micera G, Garribba E (2010) Inorg Chem 49:174–187
62. Willsky GR, Chi LH, Godzala M III, Kostyniak PJ, Smee JJ, Trujillo AM, Alfano JA, Ding W, Hu Z, Crans DC (2011) Coord Chem Rev 255:2258–2269
63. Rivadeneira J, Di Virgilio AL, Barrio DA, Muglia CI, Bruzzone L, Etcheverry SB (2010) Med Chem 6:9–23
64. Saxena AK, Srivastava P, Kale RK, Baquer NZ (1993) Biochem Pharmacol 45:539–542
65. Sabbioni E, Pozzi G, Devos S, Pintar A, Casella L, Fischbach M (1993) Carcinogenesis 14:2565–2568
66. Mukhtiar M, Khan MF, Jan SU, Khan H, Ullah N, Asim-ur-Rehman N (2012) Pak J Pharm Sci 25:549–553
67. Silvestri F, Ribatti D, Nico B, Silvestri N, Romito A, Dammacco F (1995) Ann Ital Med Int 10:7–13
68. Goncalves AP, Videira A, Soares P, Maximo V (2011) Life Sci 12:11–12
69. Montiel-Davalos A, Gonzalez-Villava A, Rodriguez-Lara V, Montano LF, Fortoul TI, Lopez-Marure R (2012) J Appl Toxicol 32:26–33
70. Zhao Y, Ye L, Liu H, Xia Q, Zhang Y, Yang X, Wang K (2010) J Inorg Biochem 104:371–378
71. Hosseini MJ, Seyedrazi N, Shahraki J, Pourahmad J (2012) Adv Biosci Biotechnol 3:1096–1103
72. Afeseh Ngwa H, Kanthasamy A, Anantharam V, Song C, Witte T, Houk R, Kanthasamy AG (2009) Toxicol Appl Pharmacol 240:273–285
73. Wu Y, Ma Y, Xu Z, Wang D, Zhao B, Pan H, Wang J, Xu D, Zhao X, Pan S, Liu L, Dai W, Jiang H (2014) Cancer Lett 351:108–116
74. Ray RS, Rana B, Swami B, Venu V, Chatterjee M (2006) Chem Biol Interact 163:239–247
75. Fu Y, Wang Q, Yang XG, Yang XD, Wang K (2008) J Biol Inorg Chem 13:1001–1009
76. Garg A, Aggarwal BB (2002) Leukemia 16:1053–1068
77. Mantovani A, Marchesi F, Portal C, Allavena P, Sica A (2008) Adv Exp Med Biol 610:112–127
78. Linnewiel-Hermoni K, Motro Y, Miller Y, Levy J, Sharoni Y (2014) Free Radic Biol Med 75:105–120
79. Divya CS, Pillai MR (2006) Mol Carcinog 45:320–332
80. Micheau O, Tschopp J (2003) Cell 114:181–190
81. Mo XM, Chen ZF, Qi X, Li XT, Li J (2012) Bioinorg Chem Appl 75:63–74
82. Katkar P, Coletta A, Castelli S, Sabino GL, Couto RA, Ferreira AM, Desideri A (2014) Metallomics 6:117–125
83. Chew ST, Lo KM, Lee SK, Heng MP, Teoh WY, Sim KS, Tan KW (2014) Eur J Med Chem 76:397–407